JACS
JOURNAL OF THE AMERICAN CHEMICAL SOCIETY
Article
pubs.acs.org/JACS

# Enhanced Raman Scattering on In-Plane Anisotropic Layered Materials

Jingjing Lin,[†] Liangbo Liang,[‡,§] Xi Ling,[∥] Shuqing Zhang,[†] Nannan Mao,[†] Na Zhang,[†] Bobby G. Sumpter,[‡,⊥] Vincent Meunier,[§] Lianming Tong,*[,†] and Jin Zhang*[,†]

[†]Center for Nanochemistry, Beijing National Laboratory for Molecular Sciences, Key Laboratory for the Physics and Chemistry of Nanodevices, State Key Laboratory for Structural Chemistry of Unstable and Stable Species, College of Chemistry and Molecular Engineering, Peking University, Beijing 100871, PR China

[‡]Center for Nanophase Materials Sciences, Oak Ridge National Laboratory, Oak Ridge, Tennessee 37831, United States

[§]Department of Physics, Applied Physics, and Astronomy, Rensselaer Polytechnic Institute, Troy, New York 12180, United States

[∥]Department of Electrical Engineering and Computer Science, Massachusetts Institute of Technology, Cambridge, Massachusetts 02139, United States

[⊥]Computer Science & Mathematics Division, Oak Ridge National Laboratory, Oak Ridge, Tennessee 37831, United States

Supporting Information

**ABSTRACT:** Surface-enhanced Raman scattering (SERS) on two-dimensional (2D) layered materials has provided a unique platform to study the chemical mechanism (CM) of the enhancement due to its natural separation from electromagnetic enhancement. The CM stems from the charge interactions between the substrate and molecules. Despite the extensive studies of the energy alignment between 2D materials and molecules, an understanding of how the electronic properties of the substrate are explicitly involved in the charge interaction is still unclear. Lately, a new group of 2D layered materials with anisotropic structures, including orthorhombic black phosphorus (BP) and triclinic rhenium disulfide ($ReS_2$), has attracted great interest due to their unique anisotropic electrical and optical properties. Herein, we report a unique anisotropic Raman enhancement on few-layered BP and $ReS_2$ using copper phthalocyanine (CuPc) molecules as a Raman probe, which is absent on isotropic graphene and h-BN. According to detailed Raman tensor analysis and density functional theory calculations, anisotropic charge interactions between the 2D materials and molecules are responsible for the angular dependence of the Raman enhancement. Our findings not only provide new insights into the CM process in SERS, but also open up new avenues for the exploration and application of the electronic properties of anisotropic 2D layered materials.

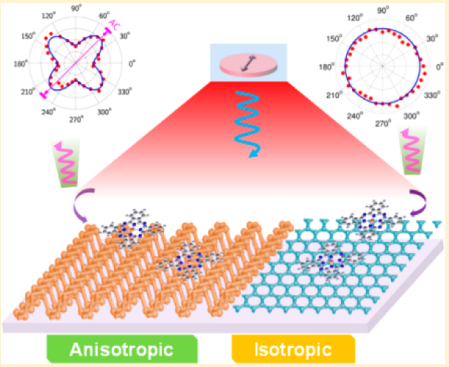


## INTRODUCTION

Since the first observation of anomalously strong Raman signals of pyridine molecules adsorbed on rough silver electrodes by Fleischmann et al. in 1974,[1] surface-enhanced Raman scattering (SERS) has been intensely studied due to its exploration as a nondestructive and ultrasensitive detection technique down to the single molecule level,[2,3] as well as its abundant and sophisticated physical/chemical processes.[4,5] In general, the electromagnetic mechanism (EM) governed by the excitation of surface plasmons[4,5] dominates the overall enhancement. The chemical mechanism (CM), which is related to the changes in the electronic polarizability of molecules, is typically several orders of magnitude lower than EM. It follows that the CM contribution is usually overwhelmed and is therefore more technically demanding to study, although a number of theoretical models have been proposed and experimental methods developed.[6−10] Recently, SERS investigations on 2D layered materials including graphene, hexagonal boron nitride (h-BN) and molybdenum disulfide ($MoS_2$) have provided a unique platform to study the CM due to its intrinsic separation from the EM effect.[11−17] The chemical enhancement involves complex processes related to the charge interactions between the molecules and the substrate, and the effects of relevant parameters have been extensively studied, including the structure and orientation of molecules,[11,16] and the energy alignment between the Fermi-level of the substrate and the HOMO/LUMO of molecules.[11,17] However, it is still not well understood how electronic properties of the substrate (besides the positions of energy bands), for example, the carrier mobility, affect the chemical enhancement of SERS, and the insight into such effects may provide a new opportunity to further reveal the fundamental processes of charge interactions and the chemical enhancement. An ideal system for this purpose requires a single material that exhibits electronic anisotropy, and on which the other parameters, such as the

Received: October 4, 2015
Published: November 19, 2015






DOI: 10.1021/jacs.5b10144
J. Am. Chem. Soc. 2015, 137, 15511−15517

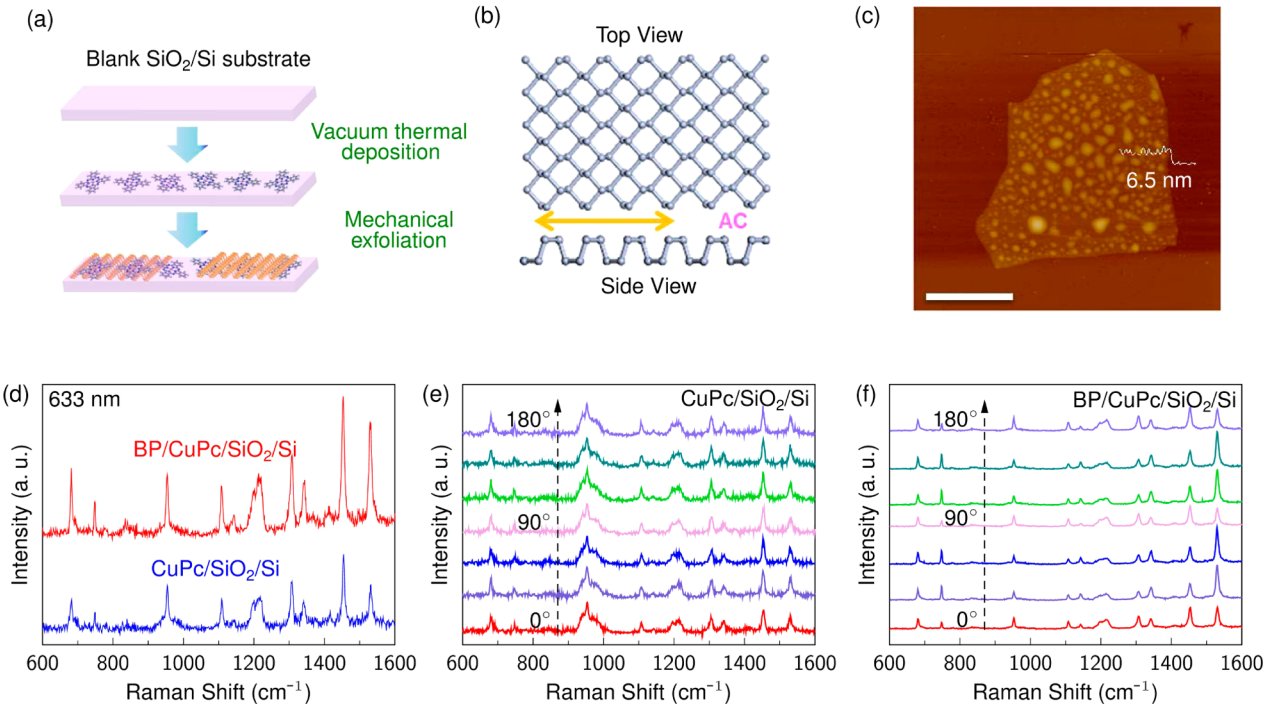


**Figure 1.** (a) Schematic illustration of the sample preparation procedure. (b) Top and side view of orthorhombic BP. The armchair direction of BP is denoted as AC and marked by the yellow double-arrow. (c) AFM image of a few-layer BP flake, where the scale bar is 2 $\mu$m. (d) Raman spectra of CuPc molecules on a 300 nm $SiO_2$/Si substrate with (red) and without (blue) few-layer BP on top. (e, f) Corresponding polarized Raman spectra of CuPc molecules on the $SiO_2$/Si substrate with (e) and without (f) BP, respectively. All the Raman spectra are collected under parallel polarization configuration with 633 nm laser for excitation.

energy alignment and molecular orientation, can be kept the same.

Lately, several new types of promising 2D layered materials with lower symmetry, including black phosphorus (BP) and rhenium disulfide ($ReS_2$), have been (re)discovered. These materials exhibit unprecedented electrical and optical properties.[18−21] More interestingly, they display unique anisotropy due to their in-plane low symmetry,[21−29] in particular, the anisotropic charge carrier mobility. In this work, by utilizing copper phthalocyanine (CuPc) molecules as a Raman probe, distinct anisotropy of Raman enhancement was found on anisotropic few-layered orthorhombic BP and triclinic $ReS_2$ substrates even though the probe molecules are randomly distributed. Such anisotropic Raman enhancement is totally absent on isotropic graphene and h-BN substrates. Since the anisotropic Raman scattering usually occurs in single-crystalline structures with finely aligned molecules,[30] our observation indicates that the anisotropy of the substrate plays an important role. To understand this specific phenomenon, Raman tensor analysis and first-principles density functional theory (DFT) calculations are performed. For BP surface, upon the contact of the CuPc molecule, the calculations suggest one-dimensional (1D) chain-like charge redistributions along armchair (AC) direction due to the highest charge carrier mobility along this direction;[22,26−29] for $ReS_2$ surface, regardless of the CuPc's presence, its charge distributions are always primarily along the zigzag (ZZ) Re atomic chain (which is also the direction with the highest charge carrier mobility[21,23,24]). Under laser irradiation, the charge carriers are more mobile and diffuse faster along the AC direction of BP or the ZZ direction of $ReS_2$. Accordingly, the CuPc molecules with their primary axis aligned in these directions are expected to have the strongest charge interaction across the interface and thus the strongest Raman enhancement. Therefore, the polarization dependence of the Raman spectra is mainly determined by this small portion of molecules with specific relative orientation. Though the apparent overall Raman enhancement factor (EF) of CuPc molecules on BP and $ReS_2$ is below 10, given the low proportion of the effective CuPc molecules, the highest EF of single CuPc molecules from the chemical enhancement can be several times larger. These findings suggest a new way to reveal the fundamental principles of charge interactions between molecules and 2D materials, which are crucial in understanding the chemical effects of SERS, and may also suggest a spectroscopic method to explore the intrinsic electronic properties of anisotropic 2D materials.

## RESULTS AND DISCUSSION

As illustrated in Figure 1a, CuPc molecules were deposited on a clean 300 nm $SiO_2$/Si substrate through vacuum thermal evaporation, and the thickness of the deposited molecules was controlled to be 2−3 Å, corresponding to a submonolayer with randomly oriented molecules. After that, BP was transferred on top of the sample by mechanical exfoliation. The atomic structure of a single layer of BP with orthorhombic structure is shown in Figure 1b, where the armchair direction (AC) of BP crystalline is marked by the yellow double-arrow. Figure 1c shows the typical AFM image of a few-layer BP flake. Given a layer-to-layer spacing of 0.53 nm,[25] this BP flake (6.5 nm thick) is determined to be made up of 10−12 atomic layers. The CuPc molecules were excited at resonance using a 633 nm laser in all the measurements. As shown in Figure 1d, the Raman signals of CuPc molecules on BP were enhanced compared to that on the blank $SiO_2$/Si substrate. The enhancement factor was estimated to be in the range of 3−6.



DOI: 10.1021/jacs.5b10144
J. Am. Chem. Soc. 2015, 137, 15511−15517

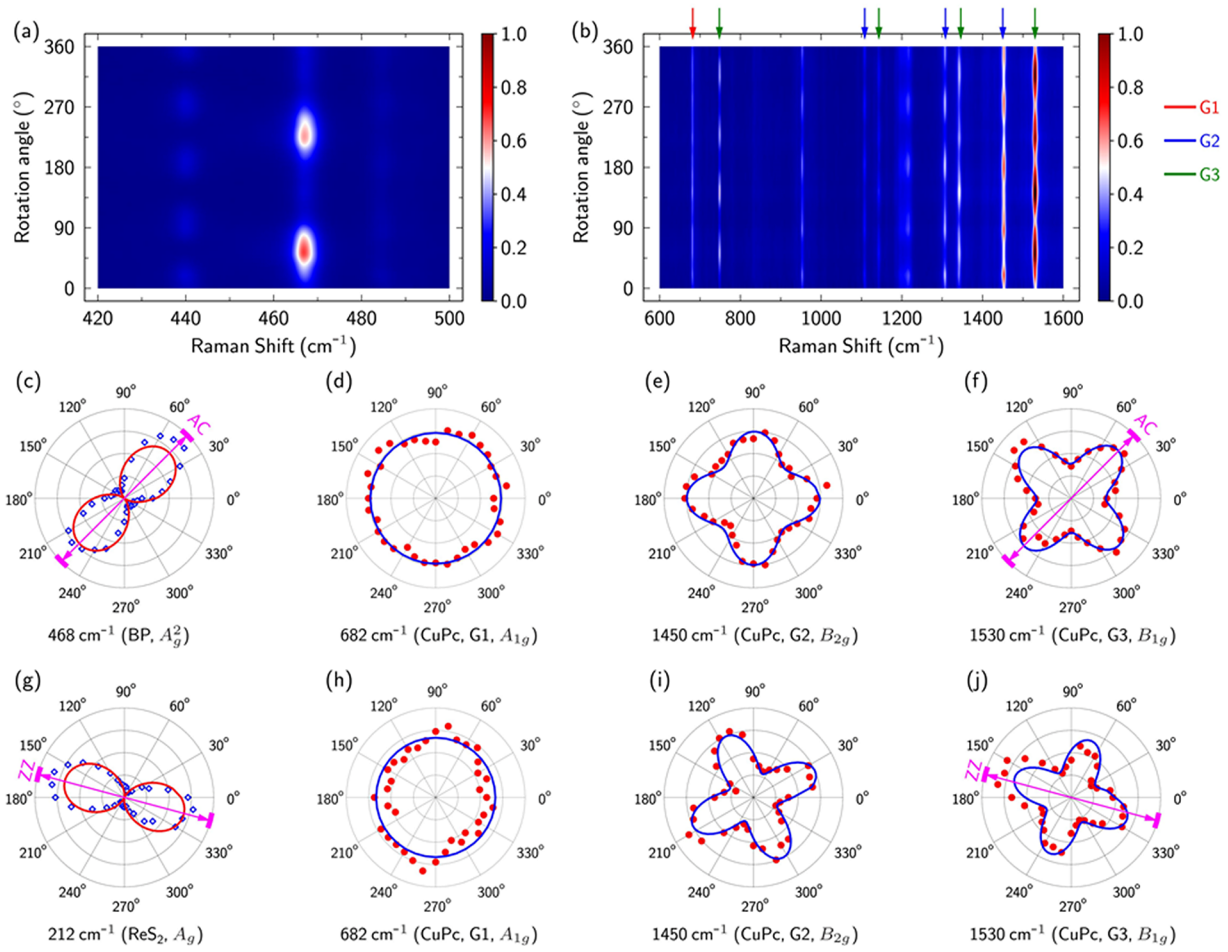


**Figure 2.** (a, b) Angular dependence of the normalized Raman spectra of BP (a) and CuPc molecules with BP (b), respectively. (c–f) Polar plots of the normalized intensities of 468 cm$^{-1}$ (BP, $A_g^2$), 682 cm$^{-1}$ (CuPc, $A_{1g}$), 1450 cm$^{-1}$ (CuPc, $B_{2g}$), 1530 cm$^{-1}$ (CuPc, $B_{1g}$) modes as a function of sample rotation angle measured on BP. (g–j) Corresponding polar plots on $ReS_2$ with its characteristic $A_g$ mode 212 cm$^{-1}$ in (g). The armchair (AC) direction of BP and the zigzag (ZZ) direction of $ReS_2$, are marked by the purple double-arrow.

In order to study the polarization dependence of the enhanced Raman spectra, angle-resolved polarized Raman spectroscopy (ARPRS) was performed on both CuPc/$SiO_2$/Si and BP/CuPc/$SiO_2$/Si structures.[21,25] The spectra were collected under parallel polarization configuration (the polarization of the incident light parallel to that of the scattered light) for all the measurements unless specifically mentioned. The sample rotation angle was defined as $\theta$. Figure 1e and 1f show the polarized Raman spectra of CuPc measured on blank $SiO_2$/Si and on the few-layer BP flake (Figure 1c) at different sample rotation angles, respectively. It can be seen that the Raman spectra of CuPc on blank $SiO_2$/Si substrate shows no polarization dependence, which confirms that the CuPc molecules were randomly distributed on the substrate. However, when measured under BP, the Raman spectra of CuPc molecules exhibited strong polarization dependence, in particular, the relative intensities of different peaks (for example, the 1450 and 1530 cm$^{-1}$ peaks) changed significantly with the sample rotation angle (Figure 1f).

The angular dependence of the Raman spectra of BP and CuPc molecules under BP at full angles is plotted in Figure 2. The plots under perpendicular polarization configuration are also shown in Figure S1 in the Supporting Information (SI). In Figure 2b, the periodic variation features of the characteristic Raman peaks of CuPc are clearly seen and can be classified into three groups, which are marked by the red, blue and green arrows, respectively. Group 1 (G1, red) includes the peak at 682 cm$^{-1}$, assigned as $A_{1g}$ mode; Group 2 (G2, blue) includes the peaks at 1450, 1308, and 1108 cm$^{-1}$, assigned as $B_{2g}$ mode; Group 3 (G3, green) includes the peaks at 1530, 1346, 1143, and 748 cm$^{-1}$, assigned as $B_{1g}$ mode. The vibrational modes of CuPc molecules are assigned according to prior references.[30−32] Figure 2c shows the polar plots of the normalized intensities of $A_g^2$ modes (468 cm$^{-1}$) of BP, indicating that the AC direction of BP is along the 45° direction,[25] as marked by the purple double-arrow. Figure 2d–f show the polar plots of the three groups of CuPc molecules as a function of the polarization angle $\theta$ in the representative of 1530, 1450, and 682 cm$^{-1}$ peaks, respectively. G1 shows no apparent polarization dependence, and both G2 and G3 exhibit a periodicity of 90° but with a phase difference of 45° between the maxima. The intensity reaches maximum (minimum) at $\theta$ = 0° (45°) for G2, while the maximum (minimum) is at 45° (90°) for G3. Interestingly, the intensity maxima of G3 coincide with the AC direction of BP. Since the CuPc molecules were deposited on the $SiO_2$/Si substrate prior to the BP transfer and were randomly oriented in a submonolayer, the angular dependence of different Raman vibrational modes should be attributed to the interplay between the CuPc molecules and BP, which we will discuss in detail below. In particular, the coincidence of the


DOI: 10.1021/jacs.5b10144
J. Am. Chem. Soc. 2015, 137, 15511−15517

AC direction and the intensity maxima of the G3 Raman modes strongly suggests that the unique anisotropic characteristic of BP plays an important role in Raman enhancement.

To confirm the contribution of the anisotropy of the substrate to the anisotropic Raman enhancement, similar experiments were carried out on few-layer $ReS_2$ (crystalline structure shown in Figure S2b). Indeed, the polarization dependence was also observed, as shown in Figure 2h–j and Figure S2–S3. In fact, the polarization dependence was the same regardless if the molecules were placed on the top or the bottom of $ReS_2$ (see in Figure S4–S5). The zigzag Re atomic chain (ZZ) direction of $ReS_2$ can be identified by the vibrational mode at 212 $cm^{-1}$,[21] marked by the purple double-arrow in Figure 2j, and thus the intensity maxima of CuPc (1530 $cm^{-1}$) now coincide with the ZZ Re atomic chain of $ReS_2$. For comparison, similar measurements were performed using isotropic graphene and h-BN as substrates. The Raman spectra at different polarization angles on graphene and h-BN are shown in Figure 3, as well as the polar plots for

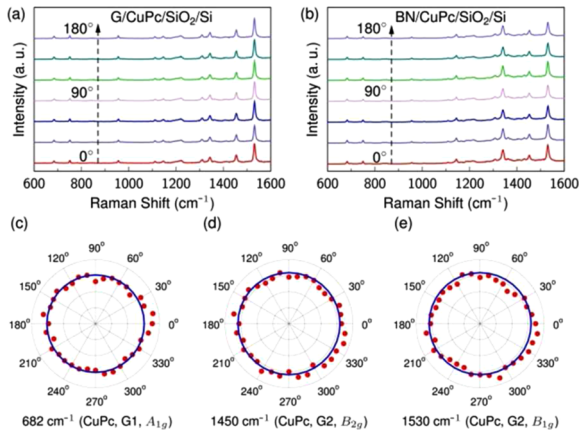


**Figure 3.** (a, b) Raman spectra of CuPc molecules on graphene and h-BN substrates with different polarization angles. (c–e) Polar plots of the normalized intensities of 682 (CuPc, $A_{1g}$), 1450 (CuPc, $B_{2g}$), and 1530 $cm^{-1}$ (CuPc, $B_{1g}$) modes as a function of the sample rotation angle.

the 682, 1450, and 1530 $cm^{-1}$ peaks of CuPc molecules. Apparently, the Raman enhancement exhibits no polarization dependent behavior. This further implies that it is the characteristic anisotropy of $ReS_2$ (or BP) rather than the orientation of the molecules that plays the determinant role in inducing the anisotropic Raman enhancement of CuPc molecules. We also measured $ReS_2$/CuPc on fused silica, and the angle dependent relative Raman intensities were also observed, indicating that this is not due to an interference effect occurring in the $SiO_2$/Si substrate.

To understand the angular dependence of the Raman spectra of CuPc on BP and $ReS_2$, we carried out a detailed group theory analysis. CuPc is a planar molecule and belongs to the $D_{4h}$ space group. The irreducible representation for the vibrational modes of CuPc molecule is as follows:[31]

$$\Gamma_{vib} = 14A_{1g} + 13A_{2g} + 14B_{1g} + 14B_{2g} + 13E_g + 6A_{1u} + 8A_{2u} + 7B_{1u} + 7B_{1u} + 28E_u \quad (1)$$

The $A_{1g}$, $B_{1g}$, $B_{2g}$ and $E_g$ modes are Raman active. The corresponding Raman tensors for the $D_{4h}$ symmetry group appear as[31]

$$A_{1g} = \begin{pmatrix} a & 0 & 0 \\ 0 & a & 0 \\ 0 & 0 & b \end{pmatrix} \qquad B_{1g} = \begin{pmatrix} c & 0 & 0 \\ 0 & -c & 0 \\ 0 & 0 & 0 \end{pmatrix}$$

$$B_{2g} = \begin{pmatrix} 0 & d & 0 \\ d & 0 & 0 \\ 0 & 0 & 0 \end{pmatrix} \quad E_{g1} = \begin{pmatrix} 0 & 0 & e \\ 0 & 0 & 0 \\ e & 0 & 0 \end{pmatrix} \quad E_{g2} = \begin{pmatrix} 0 & 0 & 0 \\ 0 & 0 & e \\ 0 & e & 0 \end{pmatrix}$$

Since the deposited CuPc molecules are in a 2–3 Å thick submonolayer, the molecules can be considered as lying flat on the substrate, which means that the plane of CuPc molecules is parallel to the surface of the substrate. Thus, we can deduce the general form of Raman tensor for CuPc molecules with a sample rotation angle $\theta$ using a transform matrix. The generalized form of Raman tensors can be expressed as

$$\widetilde{R'}(A_{1g}) = \begin{pmatrix} a(\cos^2\theta + \sin^2\theta) & 0 & 0 \\ 0 & a(\cos^2\theta + \sin^2\theta) & 0 \\ 0 & 0 & b \end{pmatrix} = \begin{pmatrix} a & 0 & 0 \\ 0 & a & 0 \\ 0 & 0 & b \end{pmatrix}$$

$$\widetilde{R'}(B_{2g}) = \begin{pmatrix} -d\sin 2\theta & d\cos 2\theta & 0 \\ d\cos 2\theta & d\sin 2\theta & 0 \\ 0 & 0 & 0 \end{pmatrix}$$

$$\widetilde{R'}(B_{1g}) = \begin{pmatrix} c\cos 2\theta & c\sin 2\theta & 0 \\ c\sin 2\theta & -c\cos 2\theta & 0 \\ 0 & 0 & 0 \end{pmatrix}$$

The tensors for the $E_g$ modes are not affected by this rotation and retain their isolated molecule description.

In general, the Raman intensity can be expressed as a function of molecule orientation and polarization geometry as follows:

$$I \propto |e_i \cdot \tilde{R} \cdot e_s|^2 \quad (2)$$

where $I$ is the collected Raman intensity, $e_i$ and $e_s$ are the unit polarization vectors of the electric field for the incident ($e_i$) and scattered ($e_s$) light, respectively. $\tilde{R}$ represents the Raman scattering tensor of a specific vibrational mode.

Considering a parallel polarization configuration, the theoretical angular dependent Raman intensity for the $D_{4h}$ symmetry group is expressed as follows:

$$I_{yy}(A_{1g}) \propto a^2 \quad (3)$$

$$I_{yy}(B_{2g}) \propto d^2 \sin^2 2\theta \quad (4)$$

$$I_{yy}(B_{1g}) \propto c^2 \cos^2 2\theta \quad (5)$$

Following eqs 3–5, the simulated polarization dependence profiles of Raman intensities are shown in Figure S6. It can be seen that the $A_{1g}$ mode shows no polarization dependence, consistent with the experimentally observed trend of G1 (Figure 2d and 2h). In contrast, the intensities of the $B_{2g}$ and $B_{1g}$ modes change with $\theta$ in a 90° periodicity. Further, the angle between the maxima of these two modes is 45°, agreeing very well with the experimental observations for G2 and G3 in


DOI: 10.1021/jacs.5b10144
J. Am. Chem. Soc. 2015, 137, 15511–15517

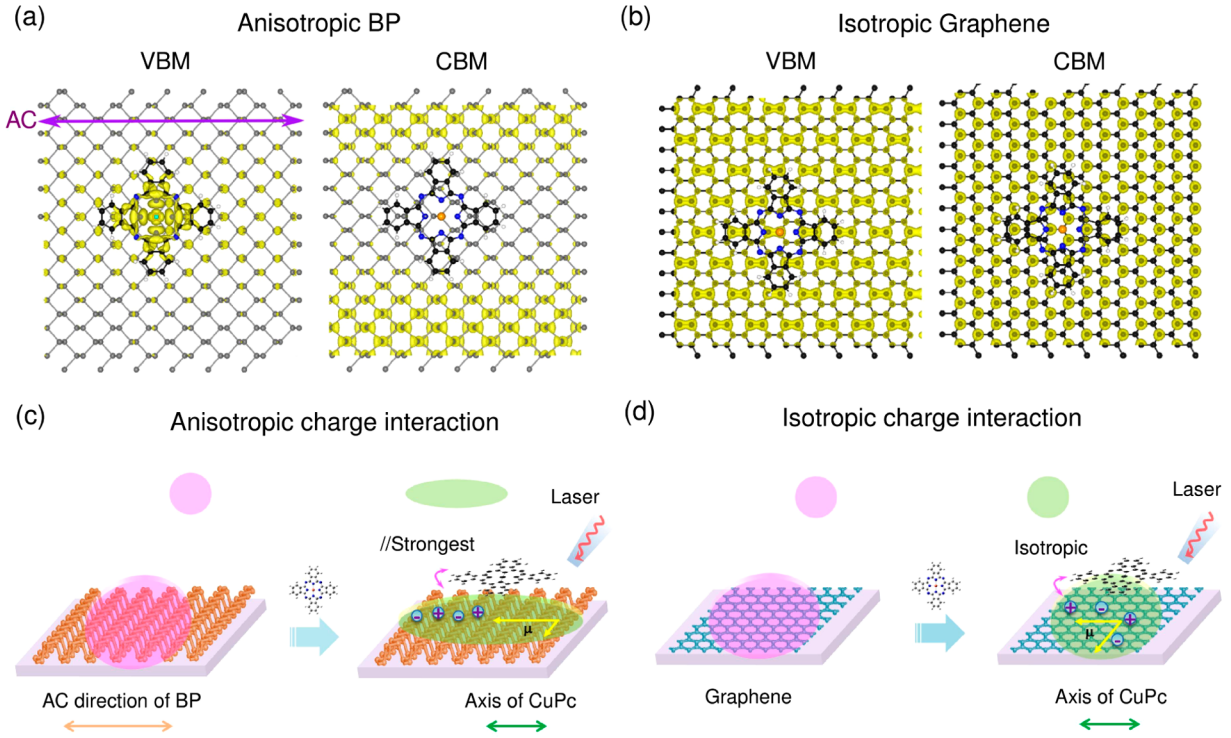


**Figure 4.** (a, b) Charge distributions (in yellow) of electronic bands near the Fermi level for (a) CuPc/BP, (b) CuPc/graphene systems. For CuPc/BP system, upon CuPc adsorption, the charges are redistributed into 1D chains along the AC direction (the direction with highest carrier mobility), while for pristine BP, the charges are uniformly distributed across the surface (see Figure S8a in SI). For graphene surface (b), even with CuPc presence, the charge distributions remain isotropic. (c, d) Schematic illustration of anisotropic and isotropic charge interaction processes in CuPc/BP (c) and CuPc/graphene (d) systems, respectively.

Figure 2e–f and 2i–j, respectively. More importantly, the group theory analysis indicates that the maximum intensity angles of the $B_{1g}$ mode correspond to the primary axis of CuPc (Figure S6c). As discussed in Figure 2, the measured maximum intensity angles of the $B_{1g}$ mode coincide with the AC direction of BP or ZZ Re chain direction of $ReS_2$. Hence, CuPc molecules contributing to the observed anisotropic polarization dependence in Figure 2 should have the primary axis aligned with the AC direction of BP or ZZ chain direction of $ReS_2$. However, we note that the simulated polarization dependence holds only for a single molecule or for a set of uniformly aligned CuPc molecules. For randomly oriented CuPc molecules that homogeneously contribute to the Raman intensities, such a polarization dependence should be smeared out. Hence, the observed polarization dependence has to be related to the anisotropy of the substrate. An orientation-dependent Raman enhancement due to the anisotropic charge interaction is proposed and discussed in detail below.

The chemical mechanism of SERS is also considered as the "electronic" enhancement[7,10] since the electrons behavior plays an important role in the enhancement. As stated above, the electron mobility of BP is the highest along the armchair direction due to the lowest effective mass of the electrons,[22,26−29] and $ReS_2$ shows the highest carrier mobility along the Re atomic chain.[21,23,24] To explore the charge interaction between CuPc molecule and BP ($ReS_2$), we performed first-principles DFT calculations for CuPc/BP, CuPc/$ReS_2$, and CuPc/graphene composite systems. According to our calculations, the interaction between CuPc and the substrate (BP, $ReS_2$, or graphene) is dominated by weak van der Waals (vdW) forces, and the average molecule−substrate separation distance is around 3.2 Å. The angle between one of the molecular branches of CuPc (primary axis) and the AC direction of BP (or ZZ of $ReS_2$) was defined as the rotation angle $\theta$. The total energies of the systems were calculated at different rotation angles and shown in Figure S7. For both CuPc/BP and CuPc/graphene systems, the energy difference for different angles is less than 50 meV (Figure S7a and S7c), indicating that the orientation of CuPc will have little effect on the charge interactions in the ground-state (without external excitations). For the CuPc/$ReS_2$ (Figure S7b) system, the energy difference is larger (~240 meV), indicating that orientation-dependent charge interactions are likely, even for the ground state.

Since Raman enhancement using 2D layered material as substrate is typically due to interfacial charge transfer and dipole interaction,[12,15−17] we also examined charge distributions of the electronic bands near the Fermi level for CuPc/BP and CuPc/graphene systems as shown in Figure 4 (CuPc/$ReS_2$ shown in Figure S9). For isolated BP, the charges are uniformly distributed across the surface for all the electronic bands near the Fermi level (see Figure S8a). However, as shown in Figure 4a, with CuPc molecules, BP's charges are redistributed into one-dimensional (1D) chains along its AC direction. More importantly, such anisotropic charge redistributions are also observed for different molecular orientations such as 0°, 30°, 45° and 60° (Figure S8).

As reported in literatures, BP has the highest carrier mobility along its AC direction.[22,26−29] The effective electron/hole mass along the AC direction is much smaller than that along ZZ direction.[26,29] This indicates that the charge carriers diffuse much faster along the AC direction. It has also been shown that


DOI: 10.1021/jacs.5b10144
J. Am. Chem. Soc. 2015, 137, 15511−15517

the photo-excited excitons in BP are highly anisotropic and are formed along the AC direction.[22,26,33] For the bare BP without external excitation, the charges show an isotropic distribution since they are bound by individual P atoms. With CuPc, the charges in the molecules interact with those in BP, which causes the redistribution of charges into the 1D chains due to the anisotropic charge mobility. For comparison, the charge distributions in graphene are both isotropic with and without CuPc molecules (Figure 4b and Figure S10). This anisotropic charge disturbance is present in BP regardless of the molecular orientation of CuPc since the energy difference is quite small for different rotation angles (Figure S7 and S8). Generally on 2D materials, the Raman enhancement was attributed to charge transfer or dipole interaction.[15] For either pathway, the strength of charge interactions also depends on the charge distribution on the substrate. Under laser excitation, anisotropic excitons are formed along the AC direction of BP,[26,33] and the charge carriers are more mobile in the AC direction. Hence, for CuPc molecules in contact with BP, the most significant charge interaction occurs only when the primary axis of CuPc is along the AC direction, as schematically shown in the Figure 4c. As a result, the molecules in such an orientation experience the strongest Raman enhancement and contribute the greatest to the total intensity. From Fermi's golden rule,[16] the matrix element for the electrons transition between the energy bands of BP and HOMO/LUMO of CuPc is the largest in this case, leading to the highest electron transition probability in the Raman scattering process. Accordingly, the Raman features are dominated by the molecules with their primary axis along the AC direction of BP and exhibit an angular dependent Raman enhancement in a similar fashion as that of a single molecule.

For the isolated $ReS_2$ surface in the distorted 1T phase,[20] it forms 1D Re atomic chains and subsequently the charges are primarily localized along the ZZ Re chain direction even without CuPc molecules, while S atoms between ZZ Re chains have little or no charge accumulation (see Figure S9a). Such anisotropic charge distributions remain after CuPc adsorption, where the molecular orientation is denoted as 0° when the primary axis of CuPc is along the ZZ Re chain direction. For other molecular orientations including 30°, 45° and 60°, similar results can be found (see Figure S9b–d). Notably, similar to the BP case, the ZZ Re chain direction along which the charges are localized is also the direction with the highest carrier mobility in $ReS_2$.[21,23,24] Similarly, charge carriers in $ReS_2$ should diffuse faster and concentrate in such a direction, resulting in the largest Raman enhancement due to the strongest charge interactions. The difference to the BP case lies in the fact that the charge distribution of $ReS_2$ without the CuPc molecules is already 1D along ZZ direction. Together with the highest carrier mobility along ZZ, the orientation-selective enhancement on $ReS_2$ is expected to be more prominent than that on BP. This might explain the narrower angular distribution of the Raman intensities of $ReS_2$, for example, the 1450 $cm^{-1}$ peak shown in Figure 2e and 2i.

For comparison, the charge distributions for a graphene surface with and without CuPc molecule were also calculated and are shown in Figure 4b and Figure S10. Since graphene has high symmetry and isotropic electronic properties, the charge distributions also remain isotropic. The charge interactions between graphene and CuPc are thus isotropic (Figure 4d). As a result, the Raman enhancement has no angular dependence, as shown in Figure 3.

## CONCLUSIONS

In summary, we investigated the angle dependent SERS effect in anisotropic 2D layered materials (both few-layered BP and $ReS_2$) using CuPc molecules as a Raman probe. An anisotropic polarization dependent Raman scattering of randomly oriented CuPc molecules was induced after interaction with few-layer BP or $ReS_2$. This observation was explored and understood in-depth with the assistance of DFT calculations. We proposed that the anisotropic electronic properties of BP and $ReS_2$, in particular, the anisotropic carrier mobility, lead to the angle-dependent Raman enhancement of CuPc molecules. We believe that more complex physics in such composite systems involving anisotropic 2D layered materials still awaits to be further explored. Nevertheless, the unique charge interactions between molecules and anisotropic 2D materials not only provide new insights into the CM process in SERS, but can also suggest new applications in optoelectronics, such as polarization-controlled molecular electronic switches.

## ASSOCIATED CONTENT

### Supporting Information

The Supporting Information is available free of charge on the ACS Publications website at DOI: 10.1021/jacs.5b10144.

Angle-resolved polarized Raman spectra of CuPc on BP ReS2 and samples (Figures S1–S5), Simulated polarization dependence for the $A_{1g}$, $B_{2g}$ and $B_{1g}$ vibrational modes of CuPc (Figures S6), DFT Calculations (Figures S7–S10). Experimental Section. (PDF)

## AUTHOR INFORMATION


### Corresponding Authors

*tonglm@pku.edu.cn

*jinzhang@pku.edu.cn


### Notes

The authors declare no competing financial interest.

## ACKNOWLEDGMENTS

This work was supported by NSFC (21233001, 21129001, 51272006, 51432002, 51121091, 11374355 and 21573004) and MOST (2011CB932601). X. L., N. N. M. and J. Z. thank the MIT international science and technology initiatives (MISTI-China) fund. The theoretical work at Rensselaer Polytechnic Institute (RPI) was supported by New York State under NYSTAR program C080117 and by the Office of Naval Research. The computations were performed using the resources of the Center for Computational Innovation at RPI. L. L. was supported as a Eugene P. Wigner Fellow at the Oak Ridge National Laboratory. B. G. S. acknowledges work at the Center for Nanophase Materials Sciences, a DOE Office of Science User Facility.

## REFERENCES

(1) Fleischmann, M.; Hendra, P. J.; McQuillan, A. J. *Chem. Phys. Lett.* **1974**, *26*, 163.

(2) Kneipp, K.; Wang, Y.; Kneipp, H.; Perelman, L. T.; Itzkan, I.; Dasari, R.; Feld, M. S. *Phys. Rev. Lett.* **1997**, *78*, 1667.

(3) Nie, S. M.; Emery, S. R. *Science* **1997**, *275*, 1102.

(4) Moskovits, M. *Rev. Mod. Phys.* **1985**, *57*, 783.

(5) Stiles, P. L.; Dieringer, J. A.; Shah, N. C.; Van Duyne, R. R. *Annu. Rev. Anal. Chem.* **2008**, *1*, 601.

(6) Persson, B. N. J.; Zhao, K.; Zhang, Z. Y. *Phys. Rev. Lett.* **2006**, *96*, 207401.



DOI: 10.1021/jacs.5b10144
J. Am. Chem. Soc. 2015, 137, 15511–15517

(7) Jensen, L.; Aikens, C. M.; Schatz, G. C. *Chem. Soc. Rev.* **2008**, *37*, 1061.
(8) Campion, A.; Ivanecky, J. E.; Child, C. M.; Foster, M. *J. Am. Chem. Soc.* **1995**, *117*, 11807.
(9) Wu, D. Y.; Duan, S.; Ren, B.; Tian, Z. Q. *J. Raman Spectrosc.* **2005**, *36*, 533.
(10) Otto, A. *J. Raman Spectrosc.* **2005**, *36*, 497.
(11) Huang, S.; Ling, X.; Liang, L.; Song, Y.; Fang, W.; Zhang, J.; Kong, J.; Meunier, V.; Dresselhaus, M. S. *Nano Lett.* **2015**, *15*, 2892.
(12) Barros, E. B.; Dresselhaus, M. S. *Phys. Rev. B: Condens. Matter Mater. Phys.* **2014**, *90*, 035443.
(13) Ling, X.; Xie, L.; Fang, Y.; Xu, H.; Zhang, H.; Kong, J.; Dresselhaus, M. S.; Zhang, J.; Liu, Z. *Nano Lett.* **2010**, *10*, 553.
(14) Ling, X.; Huang, S.; Deng, S.; Mao, N.; Kong, J.; Dresselhaus, M. S.; Zhang, J. *Acc. Chem. Res.* **2015**, *48*, 1862.
(15) Ling, X.; Fang, W.; Lee, Y.-H.; Araujo, P. T.; Zhang, X.; Rodriguez-Nieva, J. F.; Lin, Y.; Zhang, J.; Kong, J.; Dresselhaus, M. S. *Nano Lett.* **2014**, *14*, 3033.
(16) Ling, X.; Wu, J.; Xu, W.; Zhang, J. *Small* **2012**, *8*, 1365.
(17) Xu, H.; Chen, Y.; Xu, W.; Zhang, H.; Kong, J.; Dresselhaus, M. S.; Zhang, J. *Small* **2011**, *7*, 2945.
(18) Li, L.; Yu, Y.; Ye, G. J.; Ge, Q.; Ou, X.; Wu, H.; Feng, D.; Chen, X. H.; Zhang, Y. *Nat. Nanotechnol.* **2014**, *9*, 372.
(19) Ling, X.; Wang, H.; Huang, S.; Xia, F.; Dresselhaus, M. S. *Proc. Natl. Acad. Sci. U. S. A.* **2015**, *112*, 4523.
(20) Tongay, S.; Sahin, H.; Ko, C.; Luce, A.; Fan, W.; Liu, K.; Zhou, J.; Huang, Y.-S.; Ho, C.-H.; Yan, J.; Ogletree, D. F.; Aloni, S.; Ji, J.; Li, S.; Li, J.; Peeters, F. M.; Wu, J. *Nat. Commun.* **2014**, *5*, 3252.
(21) Chenet, D.; Aslan, O. B.; Huang, P. Y.; Fan, C.; van der Zande, A. M.; Heinz, T. F.; Hone, J. *Nano Lett.* **2015**, *15*, 5667.
(22) He, J.; He, D.; Wang, Y.; Cui, Q.; Bellus, M. Z.; Chiu, H.-Y.; Zhao, H. *ACS Nano* **2015**, *9*, 6436.
(23) Ho, C. H.; Huang, Y. S.; Tiong, K. K.; Liao, P. C. *J. Phys.: Condens. Matter* **1999**, *11*, 5367.
(24) Liu, E.; Fu, Y.; Wang, Y.; Feng, Y.; Liu, H.; Wan, X.; Zhou, W.; Wang, B.; Shao, L.; Ho, C.-H.; Huang, Y.-S.; Cao, Z.; Wang, L.; Li, A.; Zeng, J.; Song, F.; Wang, X.; Shi, Y.; Yuan, H.; Hwang, H. Y.; Cui, Y.; Miao, F.; Xing, D. *Nat. Commun.* **2015**, *6*, 6991.
(25) Wu, J.; Mao, N.; Xie, L.; Xu, H.; Zhang, J. *Angew. Chem., Int. Ed.* **2015**, *54*, 2366.
(26) Wang, X.; Jones, A. M.; Seyler, K. L.; Vy, T.; Jia, Y.; Zhao, H.; Wang, H.; Yang, L.; Xu, X.; Xia, F. *Nat. Nanotechnol.* **2015**, *10*, 517.
(27) Qiao, J.; Kong, X.; Hu, Z.-X.; Yang, F.; Ji, W. *Nat. Commun.* **2014**, *5*, 4475.
(28) Xia, F.; Wang, H.; Jia, Y. *Nat. Commun.* **2014**, *5*, 4458.
(29) Fei, R.; Yang, L. *Nano Lett.* **2014**, *14*, 2884.
(30) Basova, T. V.; Kiselev, V. G.; Schuster, B.-E.; Peisert, H.; Chasse, T. *J. Raman Spectrosc.* **2009**, *40*, 2080.
(31) Basova, T. V.; Kolesov, B. A. *J. Struct. Chem.* **2000**, *41*, 770.
(32) Liu, Z.; Zhang, X.; Zhang, Y.; Jiang, J. *Spectrochim. Acta, Part A* **2007**, *67*, 1232.
(33) Vy, T.; Soklaski, R.; Liang, Y.; Yang, L. *Phys. Rev. B: Condens. Matter Mater. Phys.* **2014**, *89*, 235319.


DOI: 10.1021/jacs.5b10144
*J. Am. Chem. Soc.* 2015, 137, 15511−15517